Sygnatura: Pol J Radiol, 2007; 72(2): 56-64

Polish Journal of Radiology
www.PolRadiol.com
ORIGINAL ARTICLE

Otrzymano: 2007.03.01
Zaakceptowano: 2007.03.26

Analysis of MRI spectrum of brain abnormalities in tuberous sclerosis complex – data from one institution

Elżbieta Jurkiewicz[1], Iwona Pakuła-Kościesza[1], Katarzyna Nowak[1], Jerzy Walecki[2], Sergiusz Jóźwiak[3]

[1] Department of Diagnostic Imaging, MR Unit, The Children's Memorial Health Institute, Warsaw, Poland
[2] Lab of Experimental Pharmacology Polish Academy of Sciences, Medical Research Center, Warsaw, Poland
[3] Department of Neurology, The Children's Memorial Health Institute, Warsaw, Poland

Author's address: Elżbieta Jurkiewicz, The Children's Memorial Health Institute, Dzieci Polskich 20st., 04-730 Warsaw, Poland, e-jurkiewicz@o2.pl

Summary

Background: Tuberous sclerosis complex (TSC) is an autosomal dominant multisystem disorder with gene loci located on chromosomes 9q34 (TSC1) and 16p13 (TSC2). Brain is the most frequently affected organ.

We retrospectively reviewed magnetic resonance features of the brain in 92 patients with tuberous sclerosis, examined in our Institute from 1997 to 2006.

Material/Methods: We analyzed MR imaging of the spectrum of supra- and infratentorial brain lesions encountered in TSC. MR examinations were performed with a 1.5 T scanner. The basic imaging protocol included axial SE T1WI, FSE PD, T2WI, FSE FLAIR images, sagittal T1,T2WI and coronal FLAIR images. Axial T1-WI contrast-enhanced images were obtained in each patient.

Results: Cortical tubers were found in 89 of the 92 patients (96.74%) and they have been located in frontal and parietal cerebral lobes predominantly. Cerebellar tubers were found in 12/92 (13.04%), cerebral white matter lesions in 34/92 patients (36.96%), subependymal nodules in 80/92 patients (86.96%) and subependymal giant cell astrocytomas in 11/92 of our patients (11.96%). Partial agenesis of corpus callosum, cortical dysplasia, cerebellar atrophy, intracranial arterial aneurysm, enlargement of ventricles and venous malformation were rare associated findings. Administration of gadolinium was useful in detecting and delineation subependymal giant cell astrocytomas - SGCAs.

Conclusions: Our study presents a wide range of MR signs and variance of the cerebral manifestations with TSC patients.

Key words: MRI • brain • tuberous sclerosis complex (TSC)

PDF file: http://www.polradiol.com/fulltxt.php?ICID=478112

Background

Tuberous sclerosis complex is a congenital neurocutaneus syndrome also known as Bourneville disease, characterized by widespread development of hamartoma in multiple organs.

Although is an autosomal dominant disorder, up to 60%-70% of affected patients have spontaneous mutations. This disorder caused by mutations in two different genes: *TSC1* on chromosome 9q34 and *TSC2* on 16p13. They code for proteins, hamartin and tuberin respectively, which are tumor suppressors. Gene mutations in either of the two TSC genes result in abnormal cell differentiation and deregulated control of cell size [1]. These cells migrated in an atypical way to the cortex, consequently in TSC there is evidence of widespread cortical disorganization and structural abnormalities throughout the brain.

Diagnostic criteria for tuberous sclerosis complex have been set out by Roach et al. [2]. Hamartomas, the hallmark

of the disease, are found in multiple organs: the brain, kidneys, lung, skin, heart. Brain is the most commonly affected organ. Four major cerebral findings are: cortical tubers, white matter abnormalities, subependymal nodules, subependymal giant cell astrocytomas – SGCAs. The most common neurological symptoms are seizures, mental retardation, autism, hyperactivity, spastic paralysis, ataxia. More than 75% of patients suffer from seizures, and 68% have mild to severe cognitive impairment. As a rule, larger and more numerous cortical tubers are associated with earlier seizure onset and more severe mental retardation [2, 3, 4].

Magnetic resonance imaging is considered as the most sensitive imaging technique which allows identification of typical and atypical findings.

Materials and methods

We retrospectively reviewed the magnetic resonance (MR) examinations of 92 patients who met the criteria necessary for a definite diagnosis of TSC.

48 were male (52.2%) and 44 female (47.8%). Their age varied from 25 days to 28 years, (mean 9.3 years).

Some findings in 30 of these patients were described in previous reports [5, 6, 7].

All exams were performed in our Institute from 1997 to 2006.

MR examinations were acquired with a 1.5T scanner. The basic imaging protocol included axial images: SE T1WI (500-670/16/1-2 [TR-repetition time/TE-echo time/excitations]), FSE PD, T2WI (15/80/3500-3800/1), FSE FLAIR (1800/13700/112/1-2) [IR-inversion time/TR/TE/excitations], sagittal T1, T2WI and coronal FLAIR images. Matrix size was 256x256 and 256x192, field of view: 22-23 mm, section thickness 4-5 mm, intersection gap 1 mm.

T1-weighted axial contrast-enhanced images were obtained in each patient (Gd-DTPA was administered intravenously in a standard dose of 0.1mmol/L per kilogram).

We presented a systematic cerebral MR evaluation and analyzed our MR examinations to record supra- and infratentorial brain lesions: cortical/subcortical tubers, white matter abnormalities, subependymal nodules (SENs), subependymal giant cell astrocytomas - SGCAs.

Partial agenesis of corpus callosum, cortical dysplasia, cerebellar atrophy, intracranial arterial aneurysm, enlargement of ventricles and venous malformation were associated findings.

We quantified the number, sites of cortical tubers in each cerebral lobe separately, reviewed all sequences and planes.

The number of white matter lesions, subependymal nodules and subependymal giant cell astrocytomas were quantified by an absolute count.

All these findings were evaluated for the presence or absence of enhancement.

The signal intensity of these lesions also was evaluated.

Results

Cortical tubers

We diagnosed cortical tubers as lesions caused by gyral expansion or distortion with abnormal signal intensity on T2WI and FLAIR sequence. Cortical/subcortical cerebral tubers were found in 89 of the 92 patients (96.74%). In 3 (3/89, 3.37%) patients tubers were unilateral (on the right hemisphere). Solely cerebral tuber was not seen.

Precisely brain location and number of cerebral tubers are presented in table 1.

A total of 1552 tubers were found in 89 patients. They were most commonly in the frontal lobes, but also in parietal, occipital and temporal lobes. 825 tubers were right-sided and 727 tubers were left-sided.

Cerebral tubers showed high signal intensity on FLAIR images in all 89 patients (100%), and in 19 cases (19/89, 21.35%) we found hypointense signal of central part of some tubers. Fig 1.

Cerebellar tubers were found in 12 of the 92 patients (13.04%), with total of 21 lesions (11 in the right and 10 in the left cerebellar hemisphere). All cerebellar tubers revealed high signal intensity in FLAIR images.

Contrast enhancement revealed no cerebral tubers, 11 (11/21,52.38%) cerebellar tubers were revealed by contrast enhancement. Fig 2.

Table 1. Location and number of supratentorial cortical tubers.

Brain lobe		right hemisphere		left hemisphere
	Total		**Total**	
Frontal lobe	421	0 – 13 (mean 4.6)	357	0 – 13 (mean 3.9)
Parietal lobe	204	0 – 8 (mean 2.2)	193	0 – 6 (mean 2.1)
Occipital lobe	89	0 – 4 (mean 0.9)	93	0 – 3 (mean 1.0)
Temporal lobe	111	0 – 4 (mean 1.2)	84	0 – 3 (mean 0.9)

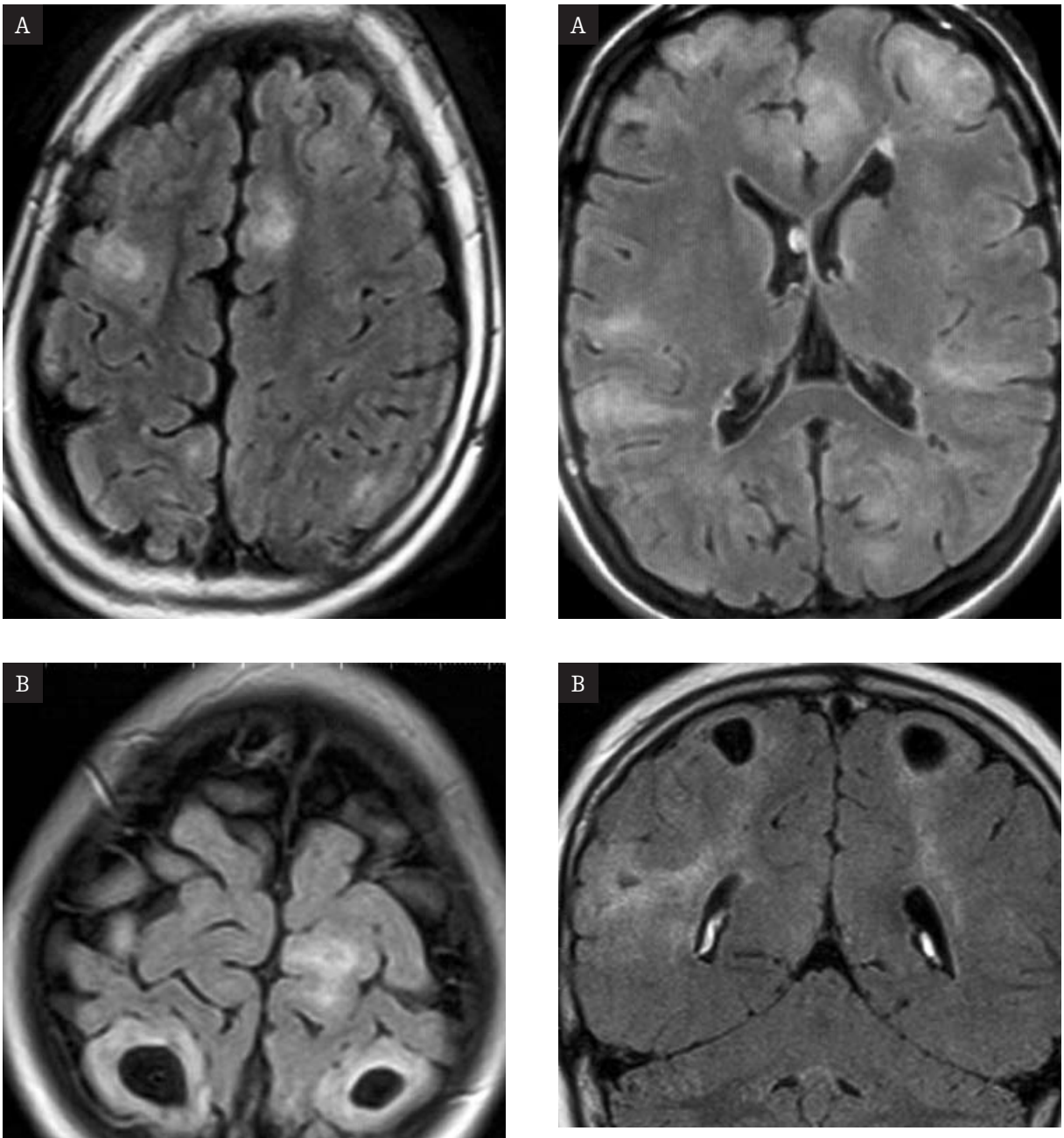

Figure 1. Cerebral cortical tubers. FLAIR sequence showed hyper- and hypointense lesions. **A** – axial image shows hyperintense signal of cortical tubers. **B** – axial and coronal images show hypointense signal of cortical tubers.

White matter abnormalities

We defined white matter lesions as linear abnormalities oriented from the ventricular wall to the cortical surface (radial bands), or presence of focal, nodular, tumeafective lesions, or as parenchymal cysts.

Cerebral white matter lesions were found in 34 of the 92 patients (36.96%).

The cerebral white matter lesions were linear with a radial distribution in 14 cases (14/34, 41.18%) and focal or tumeafective in 16 cases (16/34, 47.06%). These lesions showed hyperintensity on T2-weighted and FLAIR images.

Parenchymal cysts (also known as cyst-like white matter lesions) were found in 22 cases (22/34, 64.71%), they were round or oval with sharp contours, with signal intensities in T1, T2WI and FLAIR sequences corresponding to cerebrospinal fluid (CSF). Fig 3.

The cysts were located in the periventricular regions near the frontal and occipital horns or in deep white matter near the lateral ventricular body.

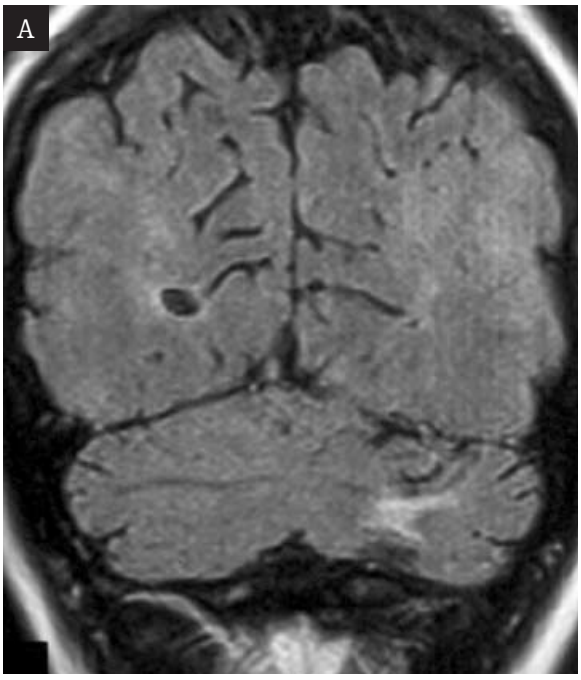

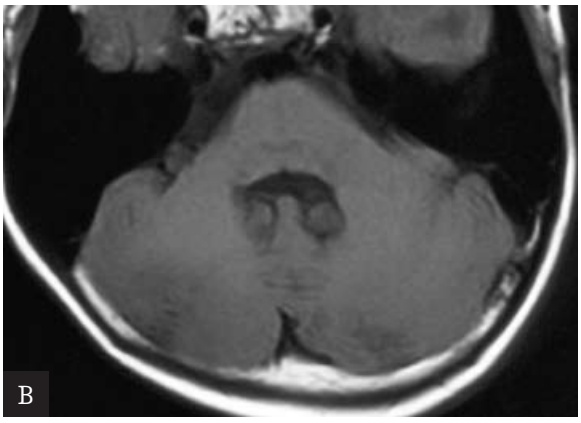

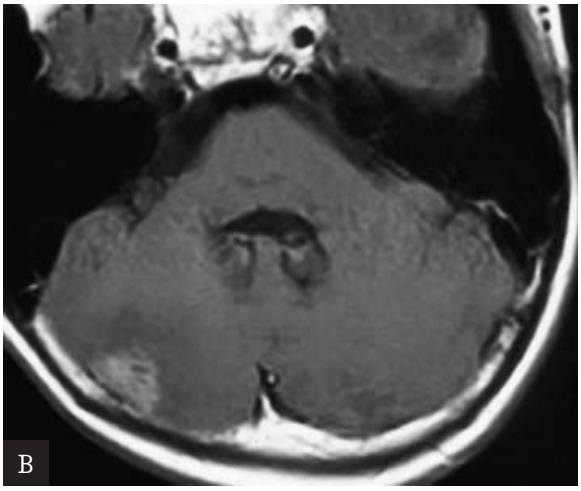

Figure 2. Cerebellar tubers. Coronal FLAIR and T1WI pre- and after contrast injection. **A** – Coronal FLAIR sequence shows cerebellar tuber with atrophy. **B** – Transverse T1-weighted image shows hypointense signal of two cerebellar tubers. Image after gadolinium injection – only one cerebellar tuber shows contrast enhancement.

Contrast enhancement was noticed in some focal, nodular white matter lesions. No enhancement of the cystic walls was seen.

Subependymal nodules – SENs

We defined SENs as lesions that originate from the ventricle walls and penetrated into the ventricle.

Subependymal nodules were detected in 80 of the 92 patients (86.96%). They were located on the lateral ventricles in all 80 patients and at the foramen of Monro in 45 cases (45/80, 56.25%). They were bilateral in 65 patients (65/80, 81.25%) and unilateral in 15 (15/80, 18.75%). SENs were 1-10 mm in diameter and did not cause obstructive hydrocephalus. The number of subependymal nodules varied from 1 to 10 per patient. They showed variably low signal intensity on T2WI and they were isointense to white matter on T1WI. Fig 4.

Most of subependymal nodules manifested nodular or ring-like enhancement.

Subependymal giant cell astrocytomas – SGCAs

We recognized subependymal giant cell astrocytomas if they were located near foramen of Monro, were larger then 12mm in diameter, caused obstructive hydrocephalus, their signal intensity was heterogenous and they revealed strong contrast enhancement.

We found SGCA in 11 from 92 of our patients (11.96%); in one case SGCA was located bilaterally. Age of patients was 5 to 14 years (mean 9.6 years). All SGCAs were located near the foramen of Monro; 5 tumors were located on the left and 7 on the right side. Fig 5

All tumors caused obstructive hydrocephalus, and contrast enhancement was observed in all cases.

The associated structural brain abnormalities were noticed as follows:

– Enlargement of lateral ventricles (without SGCAs) in 8 patients – (8/92, 8.69 %)

– Cerebellar atrophy in 6 patients – (6/92, 6.52%)

– Cortical dysplasia in 5 patients – (5/92, 5.43%)

– Partial agenesis of the corpus callosum in 3 patients – (3/92, 3.26%)

– Aneurysm of carotid artery in one patient – (1/92, 1.09%)

– Venous malformation in one patient – (1/92, 1.09%).

Discussion

MRI is the method of choice for investigating TSC and it is more sensitive than CT in identifying tubers and white matter abnormalities [8, 9].

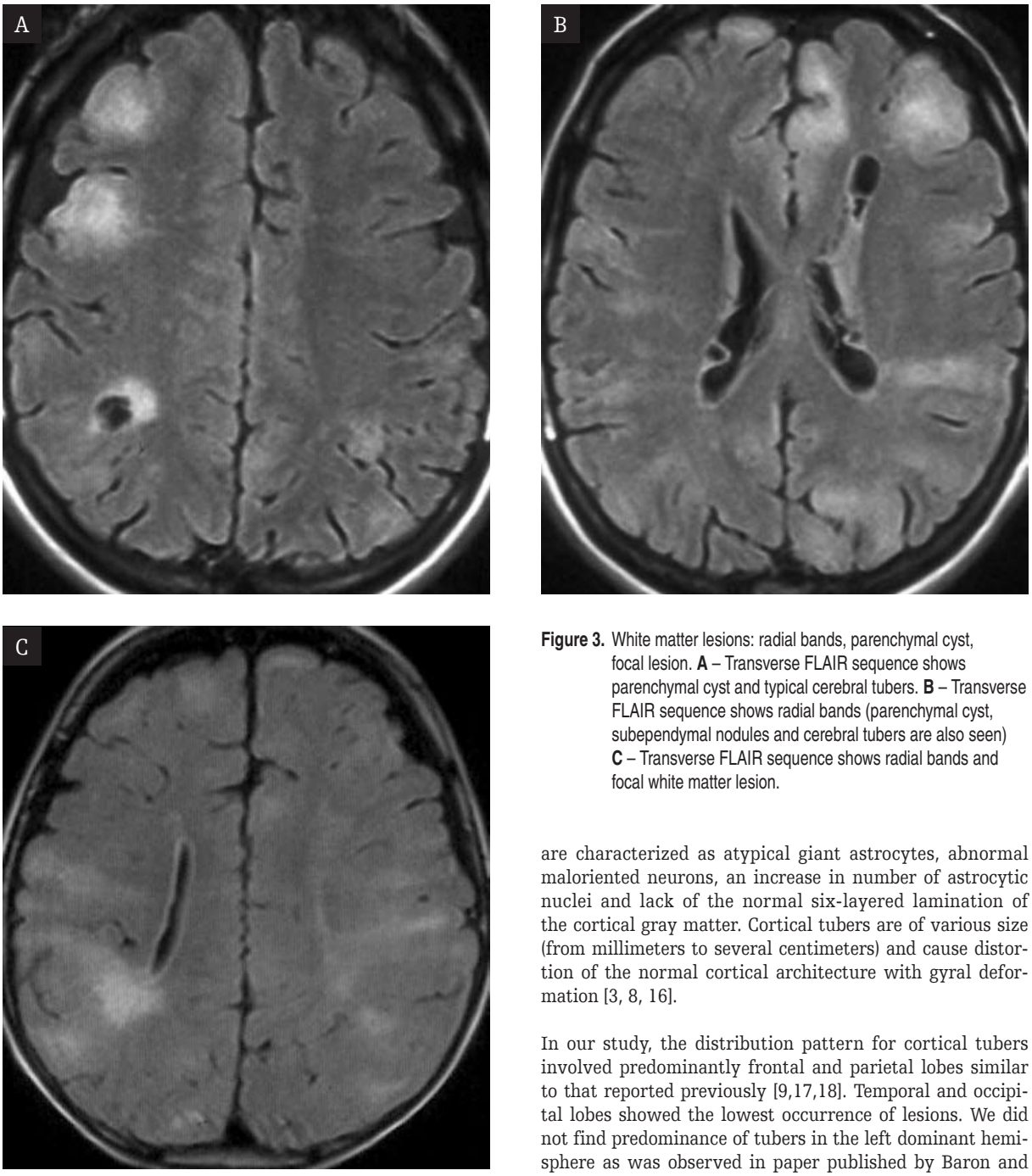

Figure 3. White matter lesions: radial bands, parenchymal cyst, focal lesion. **A** – Transverse FLAIR sequence shows parenchymal cyst and typical cerebral tubers. **B** – Transverse FLAIR sequence shows radial bands (parenchymal cyst, subependymal nodules and cerebral tubers are also seen) **C** – Transverse FLAIR sequence shows radial bands and focal white matter lesion.

Cortical tubers are the most characteristic lesions of tuberous sclerosis complex, they are detected in 88-95% of the patients, mostly in the cerebral hemispheres [8, 10, 11]. Cerebral cortical tubers are generally multiple, bilateral and mostly located in the frontal and parietal cerebral lobes. Sometimes they may be singular [12]. They can occur without cerebellar tubers, but the latter are not observed in the absence of cerebral tubers; cerebellar tubers may associate with parenchymal volume loss [8, 13, 14].

Tubers represent focal hamartomatous regions of disorganized cortical lamination [15]. Histologically, they are characterized as atypical giant astrocytes, abnormal maloriented neurons, an increase in number of astrocytic nuclei and lack of the normal six-layered lamination of the cortical gray matter. Cortical tubers are of various size (from millimeters to several centimeters) and cause distortion of the normal cortical architecture with gyral deformation [3, 8, 16].

In our study, the distribution pattern for cortical tubers involved predominantly frontal and parietal lobes similar to that reported previously [9,17,18]. Temporal and occipital lobes showed the lowest occurrence of lesions. We did not find predominance of tubers in the left dominant hemisphere as was observed in paper published by Baron and Barkovich [19].

In MR imaging a tuber was defined as a lesion affecting the cortical gray matter and adjacent white matter with an inner core hyperintense to grey and white matter on FLAIR images. Cortical tubers and white matter lesions are best seen on T2-weighted images, especially on FLAIR sequence as hyperintense areas, on T1-weighted as iso- or low-signal lesion [20, 21].

Some tubers may undergo cellular degeneration into cystic lesions, the inner part of tubers may show signal intensity that is isointense to the cerebrospinal fluid on all sequences [6, 8, 21, 22].

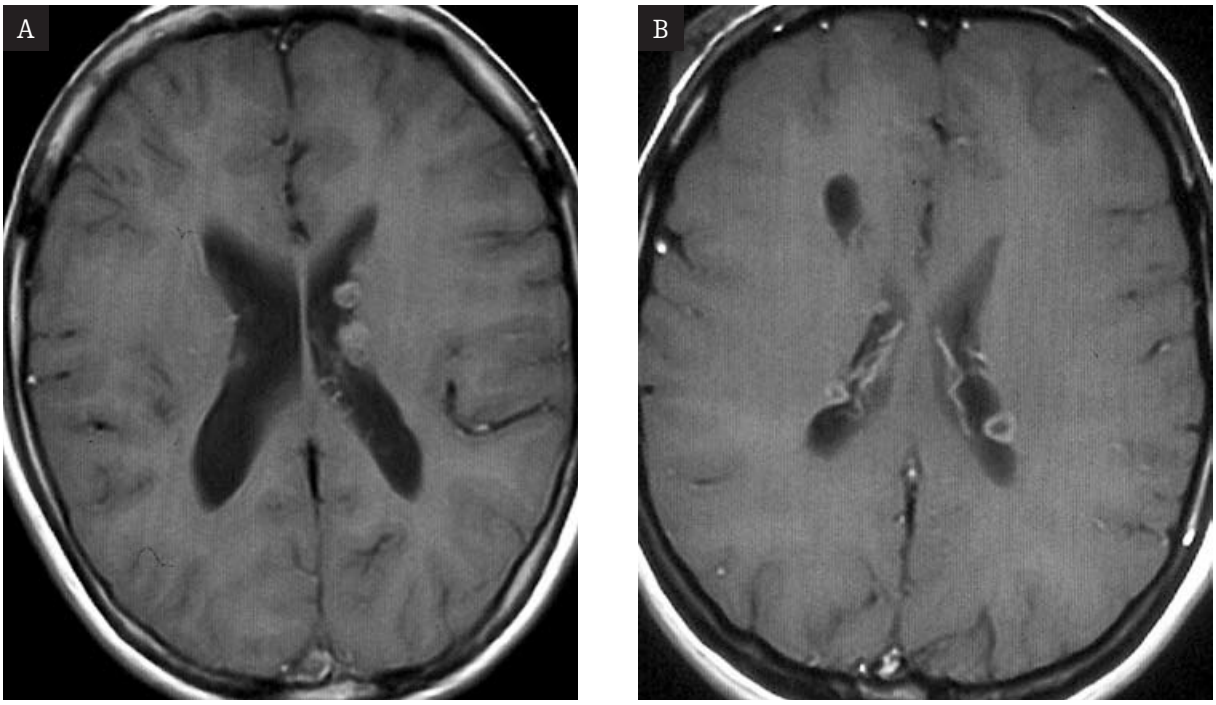

Figure 4. Subependymal nodules. **A** – Axial T1WI image before and **B**, **C** – after gadolinium injection.

Most tubers in this study of a predominantly pediatric population (average age, 9.3 years) had signal intensity (on T2WI and FLAIR images) characteristics identical to those in previous reports [10, 23].

Although in 19 patients (19/89, 21.35%) we found cyst-like cortical tubers with hypointense signal on FLAIR images, these findings were presented in our previous published paper [6].

Enhancement of cerebral tubers following contrast administration has been reported in less than 5% of patients [8].

None of supratentorial tubers in our series revealed contrast enhancement.

Cerebellar localization is less frequent and occurs in 10-15% of patients according to previous data [3, 8, 11, 24]. Only Mart-Bonmati [14] observed cerebellar lesions in 44.1% of patients (15/34). In our study cerebellar findings were disclosed in 12 of 92 patients (13.04%).

After gadolinium administration they show variable enhancement, some enhance mildly, but some of them may not enhance at all.

In our studies we noticed wegde-shaped enhancement of 11 cerebellar tubers, but 10 cerebellar tubers did not enhance. Sener [24] presented four patients with cerebellar tubers, 3 of them had contrast injection and none of the tubers enhanced. Girard [25 investigated 21 patients, all of them had gadolinium injection, only two patients presented enhancement of cerebellar tubers. Castillo [26] reported one case with three different sites of contrast enhancement in the cerebellum. He observed gyriform enhancement of a cerebellar tuber; this type of enhancement was not found in our study.

White matter abnormalities were defined as areas of abnormal signal intensity in the white matter subjacent to a tuber or nodule, linear (i.e. radial band) or wedge-shaped lesions extending from the ventricular surface to a cortical tuber and deep white matter cysts [27].

Signal intensity of white matter lesions correlated with histopathologic features, which are nearly identical in both

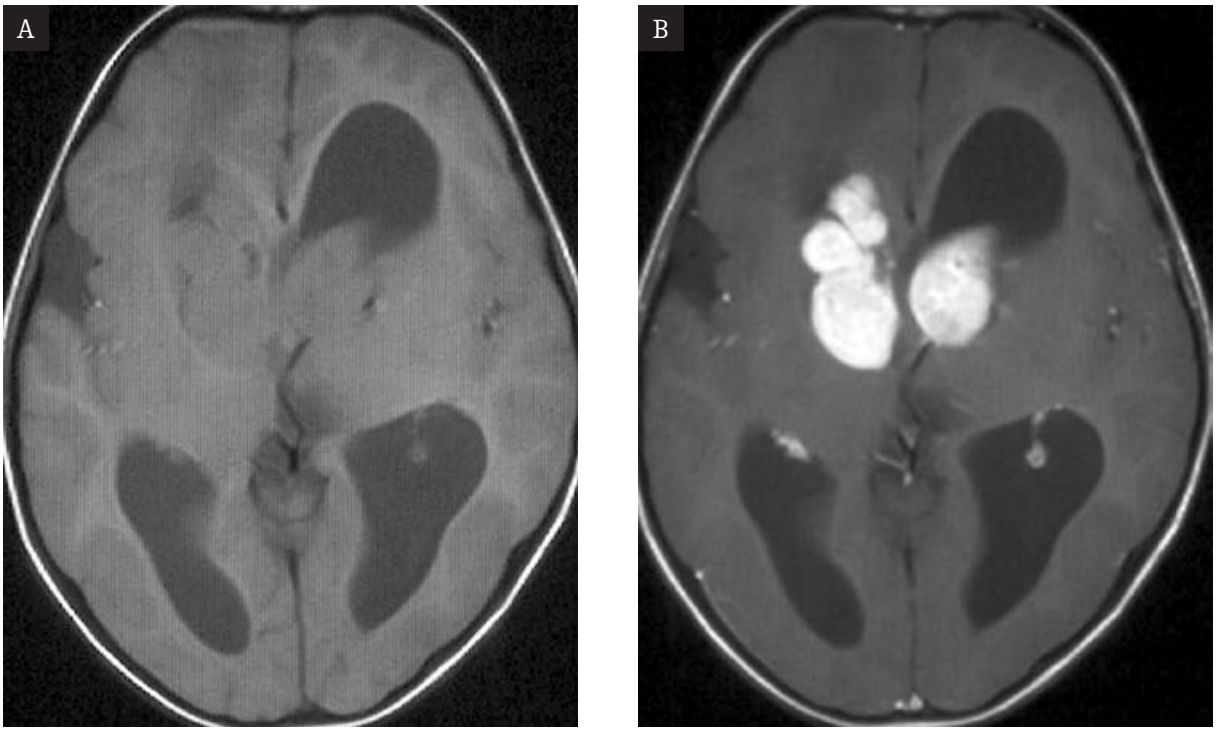

Figure 5. Subependymal giant cells astrocytoma. **A** – Axial T1WI pre- and **B** – post-contrast images show bilateral tumors.

cortical tubers and white matter abnormalities (gliosis, myelinization defects, heterotopic giant cells) [3].

Pathologic examination showed giant cells following the path of neuronal migration tracts [8, 27].

Radial bands are thought to represent a disturbance in normal migration of neural progenitor cells from the ventricular germinal matrix to the cerebral cortex during brain development.

Visualization of radial bands may be helpful in distinguishing TSC from demyelinating lesions, infections or ischemic changes [27].

White matter lesions have been reported less frequently on MR images. DiMario [21] reported white matter lesions in 30% of TSC patients, in study presented by Shepard et al. [4] 21% of patients showed linear or curvilinear lesions in the white matter, extending from subependymal nodules to cortical tubers.

Girard et al. [25] found white matter lesions in 19 of the 21 examined patients.

Only in paper published by Herron et al. [11] white matter lesions were visible in 90% of patients.

We found white matter abnormalities in 34 of 92 (37%) patients.

In our studies T2WI and FLAIR sequences showed hyperintense radially oriented white matter bands extending from the periventricular region to the cortical tubers and probably corresponding to the so-called migration lines or wedge-shaped lesions [3, 28].

Approximately 12% of these lesions show contrast enhancement [3]. We noticed contrast enhancement in 6 patients (6/34, 17.65%).

Cystic white matter lesions have recently been described as a feature of tuberous sclerosis [22].

22 patients in our sample presented parenchymal cysts; the origin of the cysts is unknown and might represent enlarged Virchow-Robin perivascular spaces, neuroepithelial cysts, or even the cystic degeneration of dysplastic lesions of white matter [22]. The cysts are most frequently located in the perivascular white matter and they are part of the spectrum of TSC lesions.

According to previously published papers we also found cyst-like lesions predominantly located in the deep white matter and near frontal and occipital horns [22, 23, 29]. In our patients no cysts were noticed within corpus callosum, unlike the studies by Van Tassel et al. [22] who reported two patients with cysts in that location.

Subependymal nodules and SEGAs are defined by their anatomic location adjacent to the ventricles of the brain and they are histologically benign lesions. The distinction between subependymal nodules and SGCAs is made on the basis of size, although there are possibly unknown genetic changes that drive the production of SGCAs from subependymal nodules [30].

Subependymal nodules (SENs) were defined as small nodular lesions originating from the wall of the lateral ventricles and protruding into the ventricular lumen. They are typically found along the ventricular surface of lateral ventricle (near the sulcus terminalis)

posterior to the foramen of Monro. However, they can also be seen elsewhere in the ventricular system.

Subependymal nodules are observed in 90%-95% of all cases [8, 10, 11]. We revealed SENs in 80 from 92 our patients (87%)

Histologically the nodules are composed of giant cells with glial and neural features and can contain many vascular elements [3]. Calcification commonly increases with age.

T1 and T2-weighted MR images are used to identify subependymal nodules which protrude into the ventricle. Subependymal nodules compared with cortical gray matter are often isointense to hyperintense on T1WI and isointense to hypointense (because of the calcification) on T2WI. 30-80% of subependymal nodules show contrast enhancement [8].

SENs may undergo neoplastic change to subependymal giant cell astrocytoma in approximately 8% of patients [31].

All SENs that we found were located in lateral ventricles, no nodules were found in third and fourth ventricle. According to previous papers they showed the same signal intensity while most of them were characterized by nodular or ring-like enhancement [8, 10, 11].

Subependymal giant cell astrocytomas are the most common brain tumors associated with TSC. Most often they are located near the foramen of Monro, less frequently in the ependymal tissue near the atria, temporal horns or very rarely in the cerebral hemisphere. Their enlargement usually leads to CSF flow obstruction. The incidence in TSC is about 5-10% [8, 32] or up to 15% according to Herron et al. [11].

The peak age of occurrence is in patients aged 8-18 years; in our study patients were aged 5–13 (average, 9.1 years).

It is believed that subependymal giant cell tumors originate from subependymal nodules.

On MR imaging SGCAs resembles SENs, except that the tumors are larger, usually heterogenous, cause hydrocephalus and show enhancement after contrast administration.

We found SGCA in 11 from 92 of our patients (11.96%). In all cases the tumors were located near the foramen of Monro, in 1 patient bilaterally.

Contrast enhancement of brain abnormalities in TSC patients indicates lack of an intact blood-brain barrier.

Gadolinium administration is not useful in detecting cortical tubers, white matter lesions and subependymal nodules, although may help in detection of SGCA; however, the parameters of size (> 12 mm), growth over the time, location and potential for obstructive hydrocephalus are also important for a presumptive diagnosis of these tumors.

Enlargement of lateral ventricles is usually caused by atrophy or repeated seizures associated with hypoxia, and it was observed in 25% cases in the study by Braffman et al. [8]. In our group of patients mild ventriculomegaly was found only in 18 patients (18/92, 19.57%)

Cerebellar tissue atrophy was also observed in a small number of our patients (only 6/92, 6,52%) similarly to data in literature; Marti-Bonmati et al. [14] observed parenchymal volume loss in 4 of 34 children (11.8%).

Cortical dysplasia was detected in 5 of our patients (5/92, 5.43%), and according to the articles published previously cortical dysplasia in those cases also encompased large segment of cortex [3, 28, 33].

We did not find hemimegalencephaly or schizencephaly associated with TSC. It is a very uncommon finding in this disease. Up to now only two cases with schizencephaly in TSC have been reported [28, 33].

According to our knowledge 7 patients with hemimegalencephaly were reported previously, one of them was the focal hemimegalencephaly [34, 35, 36, 37, 38, 39].

Partial agenesis of corpus callosum has been reported before [3, 28, 40].

We also found partial but not complete agenesis of corpus callosum in 3 patients.

Vascular lesions (stenoses, ectasia, aneurysm) are not common; they have been found predominantly in peripheral vessels. Intracerebral localization of aneurysms in TSC patients is extremely rare; the internal carotid artery is involved most commonly (60%). According to our knowledge, only 17 TSC patients with intracranial aneurysms have been previously described, one of them was our patient (9 years-old boy) [7, 41, 42].

In one case we also found venous malformation located in the left frontal lobe in a 14-year-old girl.

Conclusions

This study presents central nervous system manifestation of various abnormalities in patients with tuberous sclerosis complex.

We would like to underline the importance of proper MRI examinations with different sequences and planes for successful diagnosis and imaging of various brain lesions in tuberous sclerosis patients.

References:

1. Curatolo P. Tuberous sclerosis: genes, brain, and behaviour. Develop Med & Child Neurol 2006; 48: 404.
2. Roach ES, Gomez MR, Northrup H. Tuberous sclerosis complex consensus conference: revised clinical diagnostic criteria. J Child Neurol 1998; 13: 624–628.
3. Inoue Y, Nemoto Y, Murata R, Tashiro T, Shakudo M, Kohno K, Matsuoka O, Mochizuki K. CT and MR imaging of cerebral tuberous sclerosis. Brain & Develop 1998; 20: 209–221.

4. Shepherd CW, Houser OW, Gomez MR. MR findings in tuberous sclerosis complex and correlation with seizure development and mental impairment. Am J Neuroradiol 1995; 16: 145–155.
5. Jurkiewicz E, Jóźwiak S, Bekiesińska-Figatowska M, Pakieła-Domańska D, Pakuła-Kościesza I, Walecki J. Cerebellar lesions in children with tuberous sclerosis complex. Neuroradiology J. 2006; 19: 577–582.
6. Jurkiewicz E, Jóźwiak S, Bekiesińska-Figatowska M, Pakuła-Kościesza I, Walecki J. Cyst-like cortical tubers in patients with tuberous sclerosis complex: MR imaging with the FLAIR sequence. Pediatr.Radiol. 2006; 36: 498–501.
7. Jurkiewicz E, Jóźwiak S. Giant intracranial aneurysm in a 9-year-old boy with tuberous sclerosis. Pediatr.Radiol. 2006; 36: 463.
8. Braffman Jr BH, Bilaniuk LT, Naidich TP, Altman NR, Post MJ, Quencer RM, Zimmerman RA, Brody BA. MR imaging of tuberous sclerosis: pathogenesis of this phakomatosis, use of gadopentetate dimeglumine, and literature review. Radiology 1992; 183: 227–238.
9. Houser OW, Gomez MR. CT and MR imaging of intracranial tuberous sclerosis. J Dermatol 1992; 19: 904–908.
10. Altman NR, Pruser RK, Post MJ. Tuberous sclerosis: characteristics at CT and MR imaging. Radiology 1988; 167: 527–532.
11. Herron J, Darrah R, Quaghebeur G. Intra-cranial manifestations of the neurocutaneous syndromes Clinic Radiol 2000; 55: 82–98.
12. Yagishita A, Arai N. Cortical tubers without other stigmata of tuberous sclerosis: imaging and pathological findings. Neuroradiology 1999; 41: 428–432.
13. O'Callaghan FJ, Harris T, Joinson C, Bolton P, Noakes M, Presdee D, Renowden D, Shiell A, Martyn CN, Osborne JP. The relation of infantile spasms, tubers, and intelligence in tuberous sclerosis complex. Arch Dis Child 2004; 89: 530–533.
14. Marti-Bonmati L, Menor F, Dosda R. Tuberous sclerosis: differences between cerebral and cerebellar cortical tubers in a pediatric population. Am J Neuroradiol 2000; 21: 557–560.
15. Crino PB, Henske EP. New developments in the neurobiology of the tuberous sclerosis complex. Neurology 1999; 53: 1384–1390.
16. Nixon JR, Miller GM, Okazaki H, Gomez MR. Cerebral tuberous sclerosis: postmortem magnetic resonance imaging and pathologic anatomy. Mayo Clin Proc 1989; 64: 305–311.
17. Ridler K, Suckling J, Higgins N, Bolton P, Bullmore E. Standardized whole brain mapping of tubers and subependymal nodules in tuberous sclerosis complex. J Child Neurol 2004; 19: 658–665.
18. Gomez MR: History of the tuberous sclerosis complex. Brain and Development 1995; 17(suppl): 55–7.
19. Baron Y, Barkowich AJ. MR imaging of tuberous sclerosis in neonates and young infants. AJNR 1999; 20: 907–916.
20. Takanashi J, Sugita K, Fujii K, Niimi H. MR evaluation of tuberous sclerosis: increased sensivity with fluid-attenuated inversion recovery and relation to severity of seizures and mental retardation. Am J Neuroradiol 1995; 16: 1923–1928.
21. DiMario F. Brain abnormalities in tuberous sclerosis complex. J Child Neurol 2004; 19: 650–657.
22. Van Tassel P, Cure JK, Holden KR Cyst-like white matter lesions in tuberous sclerosis AJNR 1997; 18: 1367–1373.
23. Inoue Y, Nakajima S, Fukuda T et al. Magnetic resonance images of tuberous sclerosis: further observations and clinical correlations. Neuradiology 1988; 30: 379–384.
24. Sener RN. Cerebellar involvement in tuberous sclerosis. Comput Med Imaging Graph 1998; 22: 63–65.
25. Girard N, Zimmerman RA, Schnur RE, Haselgrove J, Christensen K. Magnetization transfer in the investigation of patients with tuberous sclerosis. Neuroradiology 1997; 39: 523–528.
26. CastilloM, Whaley RA, Point SW. Gyriform enhancement in tuberous sclerosis simulating infarction. Radiology 1992; 185: 613–614.
27. Bernauer TA. The radial bands sign. Radiology 1999; 212: 761–762.
28. Christophe C, Sekhara T, Rypens F, Ziereisen F, Christiaens F, Dan B. MRI spectrum of cortical malformations in tuberous sclerosis complex. Brain Dev 2000; 22: 487–493.
29. Pont MS, Elster AD. Lesions of skin and brain: modern imaging of the neurocutaneous syndromes Am J Roentgenol 1992; 158: 1193–1203.
30. Ess KC. The neurobiology of tuberous sclerosis complex. Semin Pediatr Neurol 2006; 13: 37–42.
31. Shepherd CW, Scheithauer BW, Gomez MR. Subependymal giant cell astrocytoma: a clinical, pathological and flow cytometric study. Neurology 1991; 28: 864–868.
32. Tsuchida T, Kamata K, Kwamata M et al. Brain tumors in tuberous sclerosis. Childs brain 1981; 8: 271–283.
33. Huntsman RJ, Sinclair DB, Richer LP. Tuberous sclerosis with open lipped Schizencepjaly. Pediatr Neurol 2006; 34: 231–234.
34. Galluzi P, Cerase A, Strambi M, Buoni S, Fois A, Venturi C. Hemimegalencephaly un tuberous sclerosis complex. J Child Neurol 2002; 17: 677–680.
35. Sakuma H, Iwata O, Sasaki M. Longitudinal MR findings in a patients with hemimegalencephaly associated with tuberous sclerosis. Brain Dev 2005; 27: 458–461.
36. Parmar H, Patkar D, Shah J, Patankar T. Hemimegalencephaly with tuberous sclerosis: a longitudinal imaging study. Australas Radiol 2003; 47: 438–442.
37. Wolpert SM, Cohen A, Libensen MH. Hemimegalencephaly: a longitudinal MR study. Am J Neuroradiol 1994; 15: 1479–1482.
38. Griffiths PD, Gardner S-A, Smith M, Rittey C, Powell T. Hemimegalencephaly and focal megalencephaly in tuberous sclerosis complex. Am J Neuroradiol 1998; 19: 1935–1938.
39. Maloof J, Sledz K, ogg JF, Bodensteiner JB, Schwartz T, Schochet SS. Unilateral megalencepfaly and tuberous sclerosis: related disorders? Child Neurol 1994; 9: 443–446.
40. Vigliano P, Canavese C, Bobba B et al: Transmantle dysplasia in tuberous scleosis: Clinical features and surgical outcome in four children. J Child Neurol 2002; 17: 752–758.
41. Beltramello A, Puppini G, Bricolo A, Bergamo Andreis IA, El-Dalati G, Longa L, Polidoro S, Zavarise G, Marradi P. Does the tuberous sclerosis complex include intracranial aneurysms? A case report with a review of the literature. Pediatr Radiol 1999; 29: 206–211.
42. Jones BV, Tomsick TA, Franz DN. Gugliemi detachable coil embolization of a giant midbasilar aneurysm in a 19-month-old patient. AJNR 2002; 23: 1145–1148.